Electronic Supplementary Information (ESI) for

In situ TEM observation on the interface-type resistive switching by electrochemical redox reactions at a TiN/PCMO interface

Kyungjoon Baek[a,b], Sangsu Park[c], Jucheol Park[d], Young-Min Kim[a,e*], Hyunsang Hwang[b], Sang Ho Oh[a,b*]

[a]*Department of Energy Science, Sungkyunkwan University, Suwon 16419, Republic of Korea*

[b]*Department of Materials Science and Engineering, Pohang University of Science and Technology (POSTECH), Pohang 37673, Republic of Korea*

[c]*Department of Nanobio Materials and Electronics, Gwangju Institute of Science and Technology (GIST), Gwangju 61005, Republic of Korea*

[d]*Gumi Electronics and Information Technology Research Institute (GERI), Gumi 39171, Republic of Korea*

[e]*Center for Integrated Nanostructure Physics, Institute for Basic Science (IBS), Suwon 16419, Republic of Korea*

*Corresponding author. Tel.: ++82 (0)31 299 4057; Fax: ++82 (0)31 299 6505; E–mail address: sanghooh@skku.edu (S. H. Oh), youngmk@skku.edu (Y.-M. Kim)

Supplementary Text 1: Fitting analysis of *I-V* curves

To determine the conduction mechanism of the TiN/PCMO/Pt junction device, the *I-V* curves obtained from positive bias sweeps were fitted by following the various models: Poole-Frenkel emission (PFE), Schottky emission (SE), space-charge-limited current (SCLC), direct tunneling (DT) and trap assisted tunneling (TAT).[1,2] Fig. S6 shows the fitting results of an *I-V* curve according to: PFE with $\ln(I/V) \propto \sqrt{V}$, SE with $\ln(I) \propto \sqrt{V}$, SCLC with $I \propto V^2$, DT with $I \propto \sinh(V)$, and TAT with $\ln(I) \propto V^{-1}$ relation. The results show that the fitting by PFE model yields the best linearity among various models.

Supplementary Text 2: Reproducibility of *in situ* TEM experiments

A sharp increase in current during the set switching was observed also in other samples. Fig. S7 represents one example obtained from a TiN/PCMO/Pt device contained in the same wafer. The *I-V* characteristics and correlated TEM images revealed that the abrupt threshold-like switching is always accompanied by structural changes of PCMO grains with appearance of Moiré fringes. To check whether the high vacuum condition (~10^{-5} Pa) of TEM affects the observed switching behaviors, we performed a control experiment using TEM specimens with surface protection. For this purpose, we first prepared TEM samples of the TiN/PCMO/Pt device following the same procedure as the conventional method (Fig. S3) before the trench milling and final ion polishing stages. Then, 10 nm-thick SiO_2 passivation films were deposited on both sides of the TEM sample by RF sputter deposition (Fig. S8a). To make an electrical circuit, we partially shaded the Cu grid during the deposition of SiO_2 using a protection tape and also partially removed the SiO_2 passivation film deposited on the Pt top electrode using FIB. The results show that a SiO_2-passivated TEM sample exhibits the same switching behaviors as unpassivated TEM samples; the current hysteresis in a positive bias sweep (+5 V) accompanies the growth of *a*-TiO_xN_y layer (~ 10 nm in thickness) (Figs. S8b and c).

Supplementary Figures

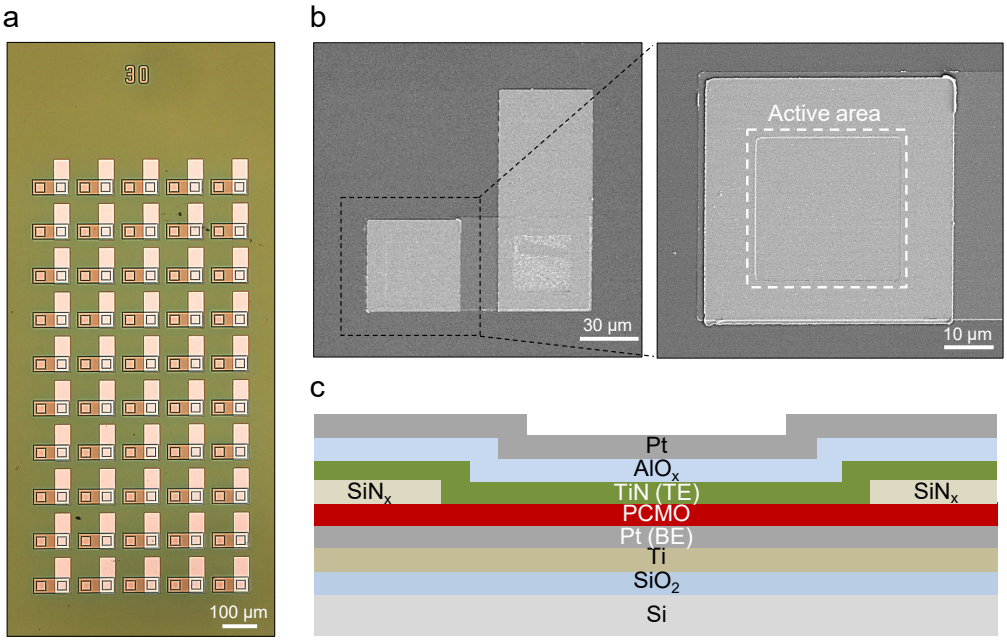

Figure S1. RRAM device array and the layer structure of TiN/PCMO/Pt junction devices. (a) An optical microscopy image of the array of TiN/PCMO/Pt junction devices. (b) SEM images of the active device area of a single device. The active device area is 30 × 30 μm^2. (c) Schematic drawing representing the layer structure of the active device area.

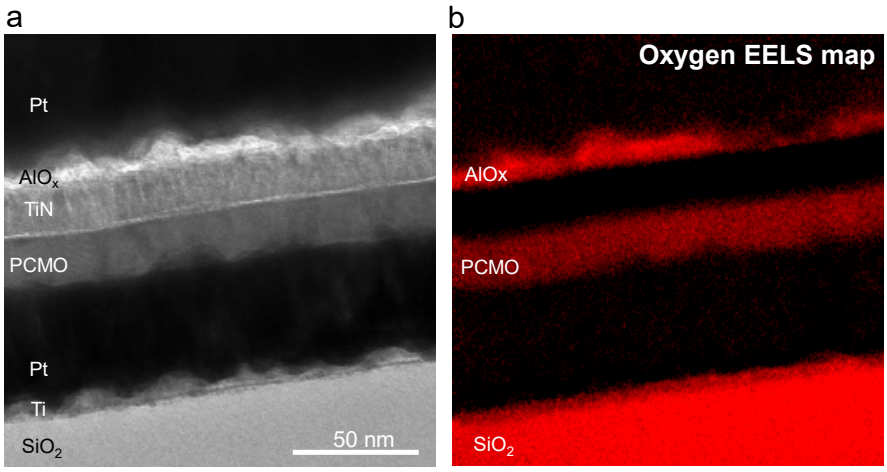

Figure S2. (a) Cross-sectional TEM image showing the layer structure of a TiN/PCMO/Pt junction device before in-situ TEM switching. (b) EELS O-K intensity map. The TEM image and the EELS map reveal that Pt and TiN are short-circuited at many locations along their interface.

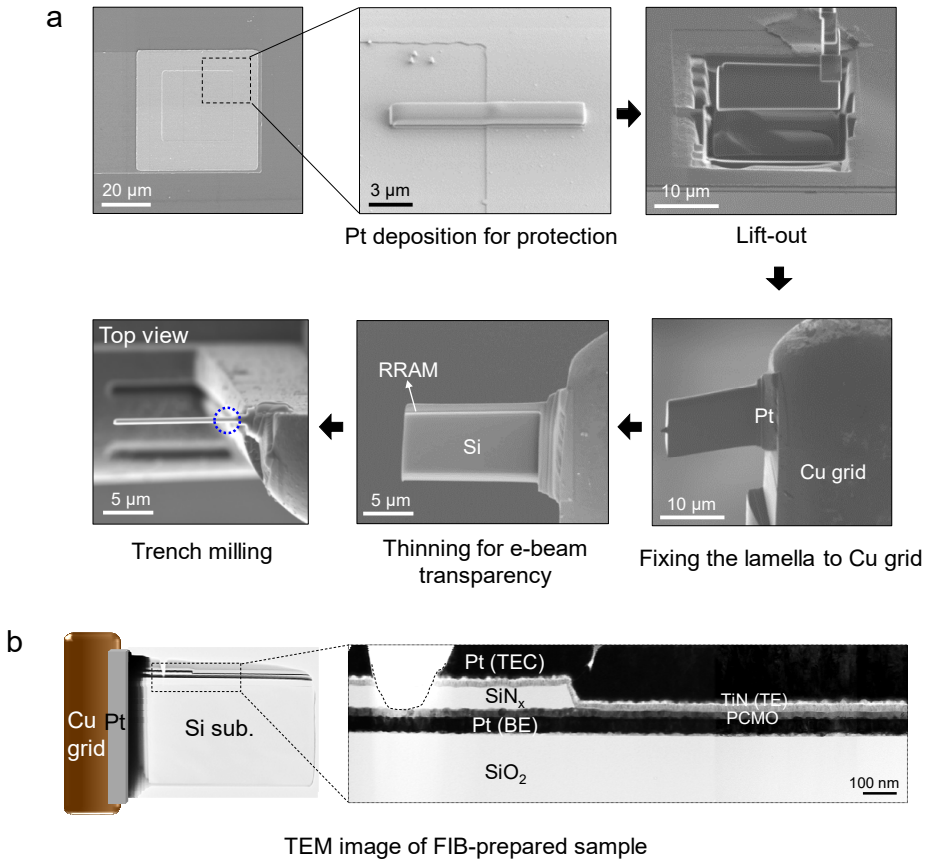

Figure S3. Preparation of the TEM specimen for *in situ* resistive switching experiments using FIB. (a) A series of SEM images illustrating the procedure of TEM sample preparation using FIB lift-out technique. The blue dotted circle marks the position where a trench was milled for the electrical isolation of the top electrode. (b) TEM bright-field image of the FIB-prepared TEM sample. A magnified view of the trench is shown on the right.

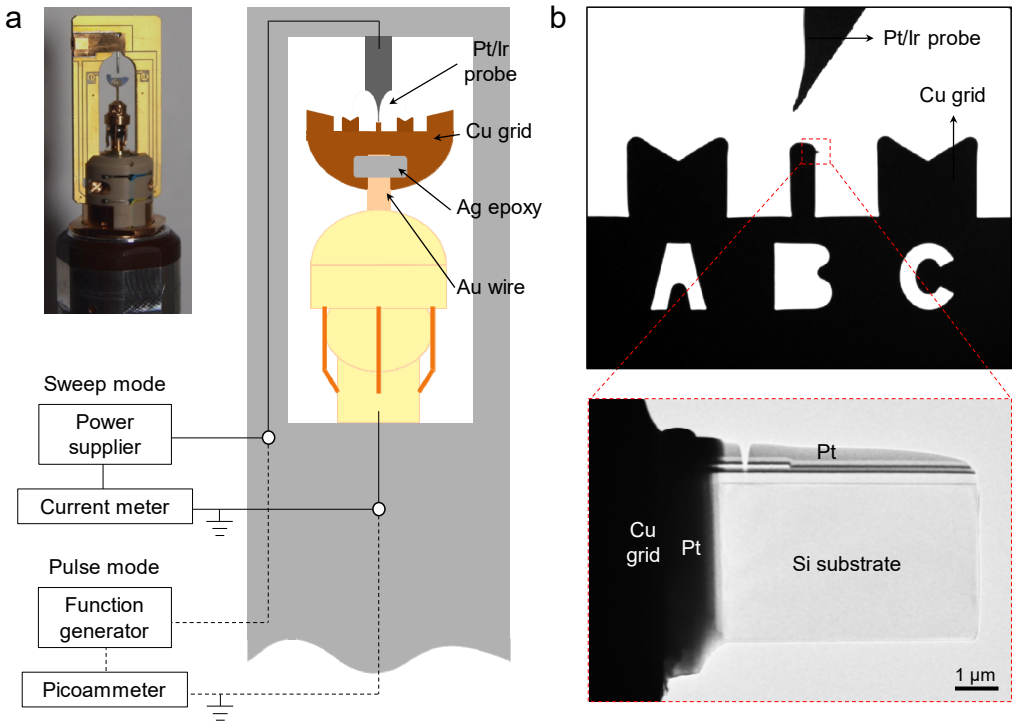

Figure S4. Experimental setup for *in situ* resistive switching in TEM. (a) STM-TEM holder and its schematic drawing illustrating the piezoelectric sample stage, the Pt/Ir probe used for electrical contact and the electrical measurement units. The switching at voltage sweep mode were carried out using the built-in Nanofactory^{TM} controller system. The switching at voltage pulse mode was conducted by connecting an external *I-V* system, including a function generator (Agilent 33250A) and a pico-ammeter (Keithley 6485). (b) TEM bright-field images showing the Pt/Ir probe and FIB-prepared TEM sample.

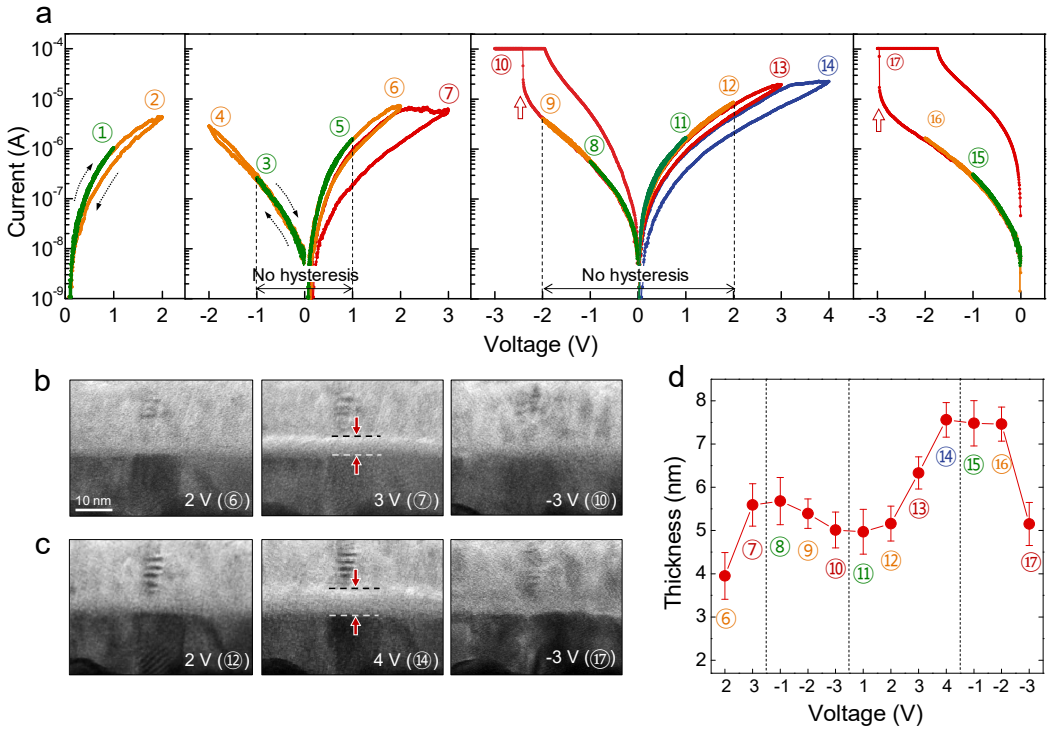

Figure S5. Change of switching behavior on multiple pass of DC bias sweeps. (a) *I-V* characteristics of a pristine state of TiN/PCMO/Pt junction device acquired with multiple pass of voltage sweeps in TEM. A series of positive and negative bias sweeps (total 17 individual bias sweeps) in an alternating order was performed with monitoring the change of the interface reaction layer thickness. (b) TEM images captured at +2 V (during the sweep no. 6), +3 V (no. 7) and -3 V (no. 10). The interfacial layer is indicated by red arrows. (c) TEM images captured at +2 V (during the sweep no. 12), +4 V (no. 14) and -3 V (no. 17). (d) Thickness of the layer measured at each peak voltage (V_{RESET}, V_{SET}) in the bias sweeps.

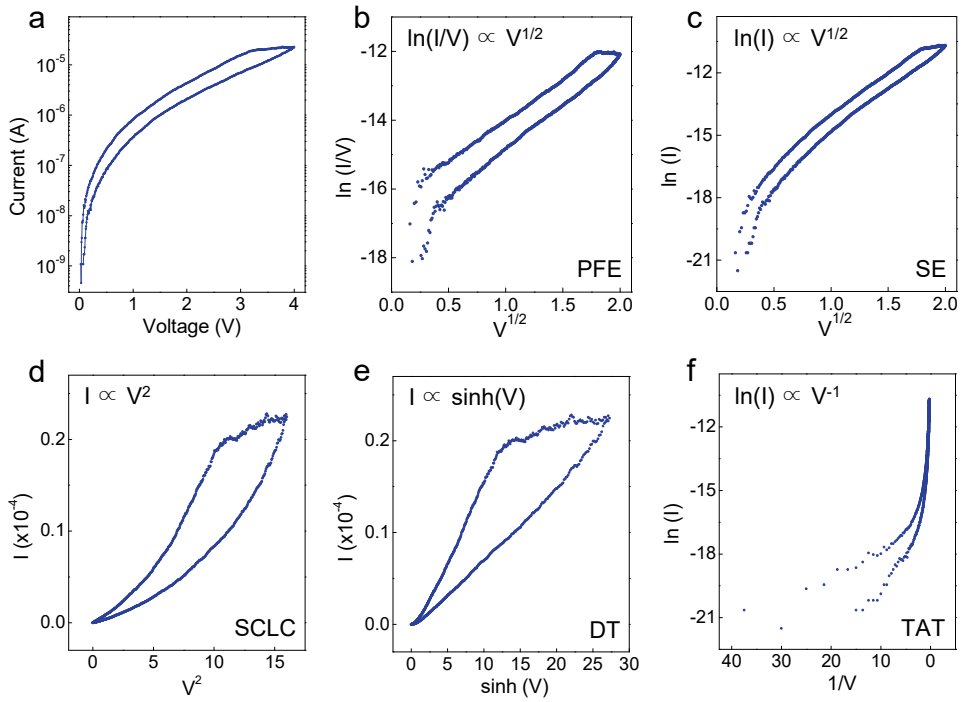

Figure S6. Fitting analysis of the measured *I-V* curves. (a) A typical *I-V* characteristic of a TiN/PCMO/Pt junction device obtained in TEM with the application of a positive bias sweep (V_{RESET} = +4 V). (b) ln *(I/V)* versus $V^{1/2}$ plot according to the Poole-Frenkel emission (PFE) mechanism. (c) ln *(I)* versus $V^{1/2}$ plot according to the Schottky emission (SE) mechanism. (d) *I* versus V^2 plot according to the space-charge-limited current (SCLC) mechanism. (e) *I* versus sinh*V* plot according to the direct tunneling (DT) mechanism. (f) ln *(I)* versus V^{-1} plot according to the trap-assisted tunneling (TAT) mechanism.

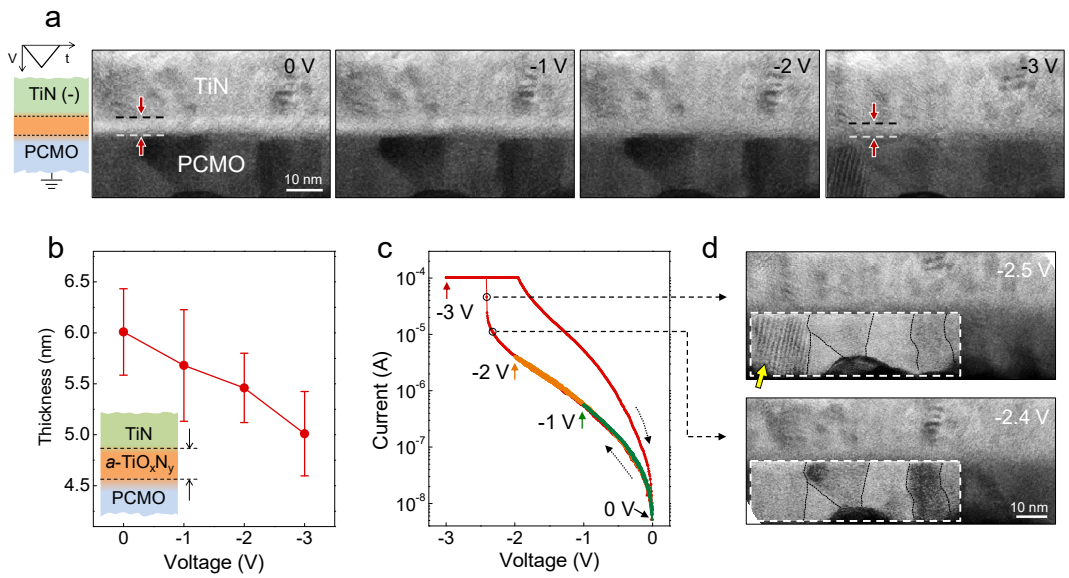

Figure S7. *In situ* TEM resistance switching to LRS via phase transition of PCMO. (a) Snapshot TEM images showing the resistive switching by interface reaction. The thickness change of *a*-TiO_xN_y layer at the V_{SET} of negative bias sweeps is marked by red arrows. (b) Plot of the thickness change of the *a*-TiO_xN_y interfacial layer versus V_{SET}. (c) Simultaneously measured *I-V* curves (log-scale) obtained during negative bias sweeps (0 V → -V_{SET} → 0 V, where V_{SET} = -1 V (green), -2 V (orange), -3 V (red)) in TEM. While the current increases continuously and shows no hysteresis until -2 V, and it increases abruptly to the current compliance at around -2.5 V. (d) Snapshot TEM images captured at -2.4 V (bottom) and -2.5 V (top) showing the microstructural changes of PCMO grains (the Moiré fringes indicated yellow arrow) during abrupt threshold-like switching at around -2.5 V. The PCMO layers outlined by white dotted lines are highlighted by enhancing the contrast.

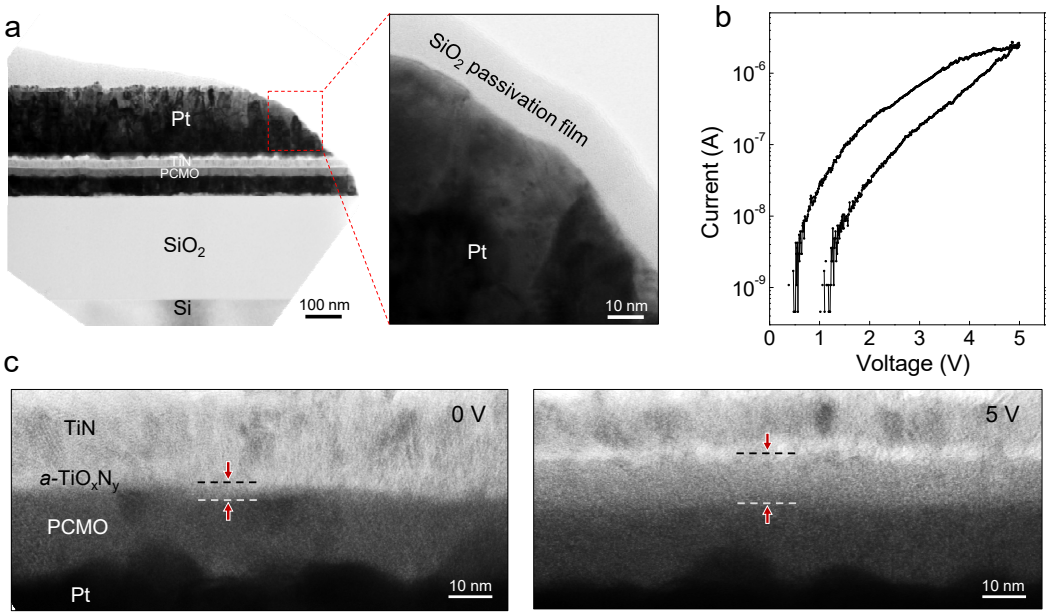

Figure S8. *In situ* TEM resistance switching of a SiO_2-passivated TEM sample. (a) TEM images of a SiO_2-passivated TEM sample of TiN/PCMO/Pt junction device. The thickness of deposited SiO_2 passivation layer is around 10 nm. (b) *I-V* characteristics of a passivated TiN/PCMO/Pt junction device obtained by *in situ* TEM. (c) Corresponding TEM images captured at 0 V (left) and at +5 V (right) in a positive bias sweep (0 V $\rightarrow$ V_{RESET} $\rightarrow$ 0 V, where V_{RESET} = +5 V).

References

1 S. Ye, X. Guan, H. S. P. Wong, *Appl. Phys. Lett.*, 2011, **99**, 063507.

2 Y. Kim, S. Ohmi, K.Tsutsui, H. Iwai, *Jpn. J. Appl. Phys.*, 2005, **44**, 4032.

Movie legends

Movie S1. The movie shows *in situ* TEM recording of a TiN/PCMO/Pt junction device during the series of positive bias sweeps ($0 \rightarrow +V_{RESET} \rightarrow 0$). The simultaneously measured *I-V* curves are included in the movie. The growth of *a*-TiO_xN_y interfacial layer is clearly observed with an increase of V_{RESET}. The thickness change of *a*-TiO_xN_y interfacial layer is marked by yellow arrows. The original movies recorded in real-time (25 fps) with a constant sweep rate (0.1 V s^{-1}) are played at various playback rates: 2 times faster for the V_{RESET} = 1 V sweep (50 fps); 4 times faster for the V_{RESET} = 2 V sweep (100 fps); 6 times faster for the V_{RESET} = 3 V sweep (150 fps); 8 times faster for the V_{RESET} = 4 V sweep (200 fps).

Movie S2. The movie shows *in situ* TEM recording of a TiN/PCMO/Pt junction device during the switching to a high resistance state by application of voltage pulses. The TEM sample was previously switched to a low resistance state. The voltage pulse has an amplitude of +3.5 V, a duration time of 3 s, and an interval time of 2 s. Total 20 pulses were applied, and the current was measured simultaneously. The current decreases gradually with an increase of the pulse number and saturates after the application of around 10 pulses. The *a*-TiO_xN_y interfacial layer grows until around 10 pulses and shows no further growth after 10 pulses. The original movie was recorded in real-time (25 fps) and played 2 times faster (50 fps).

Movie S3. The movie shows *in situ* TEM recording of the same device as in Movie S1 during the positive bias sweep ($0 \rightarrow +V_{RESET} \rightarrow 0$), where V_{RESET} is +3 V and +4 V. The TEM sample was previously switched by positive bias sweep ($0 \rightarrow +2$ V $\rightarrow 0$). The plot of the thickness variation of *a*-TiO_xN_y interfacial layer is synchronized with the movie. The partial dissolution of grown *a*-TiO_xN_y layer (indicated by yellow arrows) and the void-like contrasts (indicated by orange arrows) are observed during the ramp-down stage ($+V_{RESET} \rightarrow 0$). The original movies were recorded in real-time (25 fps) with a constant sweep rate (0.1 V s^{-1}) and played: 6 times faster for the V_{RESET} = 3 V sweep (150 fps); 8 times faster for the V_{RESET} = 4 V sweep (200 fps).

Movie S4. The movie shows *in situ* TEM recording of the same device as in Movie S1 during the negative bias sweep ($0 \rightarrow -V_{SET} \rightarrow 0$) with an increase of voltage (V_{SET}) from -1 V to -3 V. The TEM sample was previously switched to a high resistance state by positive bias sweep ($0 \rightarrow +3$ V $\rightarrow 0$). The *a*-TiO_xN_y interface layer become thinner with an increase of V_{SET} up to -2 V. At around -2.5 V, an abrupt current increase is observed with the structural changes in PCMO grains (indicated by a yellow arrow), resulting in a highly conductive state. The

original movies were recorded in real-time (25 fps) with a constant sweep rate (-0.1 V s^{-1}) and played: 2 times faster for the V_{SET} = -1 V sweep (50 fps); 4 times faster for the V_{SET} = -2 V sweep (100 fps); 6 times faster for the V_{SET} = -3 V sweep (150 fps).